



Published in final edited form as:

*Analyst.* ; 148(22): 5673–5683. doi:10.1039/d3an01487h.

## Database-assisted, globally optimized targeted secondary electrospray ionization high resolution mass spectrometry (dGOT-SESI-HRMS) and spectral stitching enhanced volatilomics analysis of bacterial metabolites†

Fouad Choueiry<sup>‡,a,b</sup>, Rui Xu<sup>‡,a</sup>, Kelly Meyrath<sup>a</sup>, Jiangjiang Zhu<sup>a,b</sup>

<sup>a</sup>Department of Human Sciences, The Ohio State University, USA.

<sup>b</sup>James Comprehensive Cancer Center, The Ohio State University, 400 W 12th Ave, Columbus, OH 43210, USA

### Abstract

Secondary electrospray ionization high-resolution mass spectrometry (SESI-HRMS) is an innovative analytical technique for the rapid and non-invasive analysis of volatile organic compounds (VOCs). However, compound annotation and ion suppression in the SESI source has hindered feature detection, stability and reproducibility of SESI-HRMS in untargeted volatilomics. To address this, we have developed and optimized a novel pseudo-targeted approach, database-assisted globally optimized targeted (dGOT)-SESI-HRMS using the microbial-VOC (mVOC) database, and spectral stitching methods to enhance metabolite detection in headspace of anaerobic bacterial cultures. Headspace volatiles from representative bacteria strains were assessed using full scan with data dependent acquisition (DDA), conventional globally optimized targeted (GOT) method, and spectral stitching supported dGOT experiments based on a MS peaks list derived from mVOC. Our results indicate that spectral stitching supported dGOT-SESI-HRMS can proportionally fragment peaks with respect to different analysis windows, with a total of 109 VOCs fragmented from 306 targeted compounds. Of the collected spectra, 88 features were confirmed as culture derived volatiles with respect to media blanks. Annotation was also achieved with a total of 25 unique volatiles referenced to standard databases allowing for biological interpretation. Principal component analysis (PCA) summarizing the headspace volatile

†Electronic supplementary information (ESI) available: Fig. S1: PLS-DA summarizing the differences in headspace chemical profiles among our bacteria cultures, media blanks and VOCQC samples. Fig. S2: Summary of dGOT method performance when incorporating three unique target list windows. Fig. S3: Representative head to tail spectra of annotated MSMS features from dGOT-SESI-HRMS analysis of bacterial headspace volatiles. Fig. S4: Principal component analyses summarizing each of DDA, GOT and DGOT method's respective ability at distinguishing the volatile differences between GutMix and each representative strain supplemented with sucrose. Fig. S5: Heatmap summarizing the relative abundance of the annotated features detected with the dGOT method across all of our culture groups. See DOI: <https://doi.org/10.1039/d3an01487h>

zhu.2484@osu.edu; Tel: +1 614-685-2226.

‡Co-first authors, these authors contributed equally to this project.

Author contributions

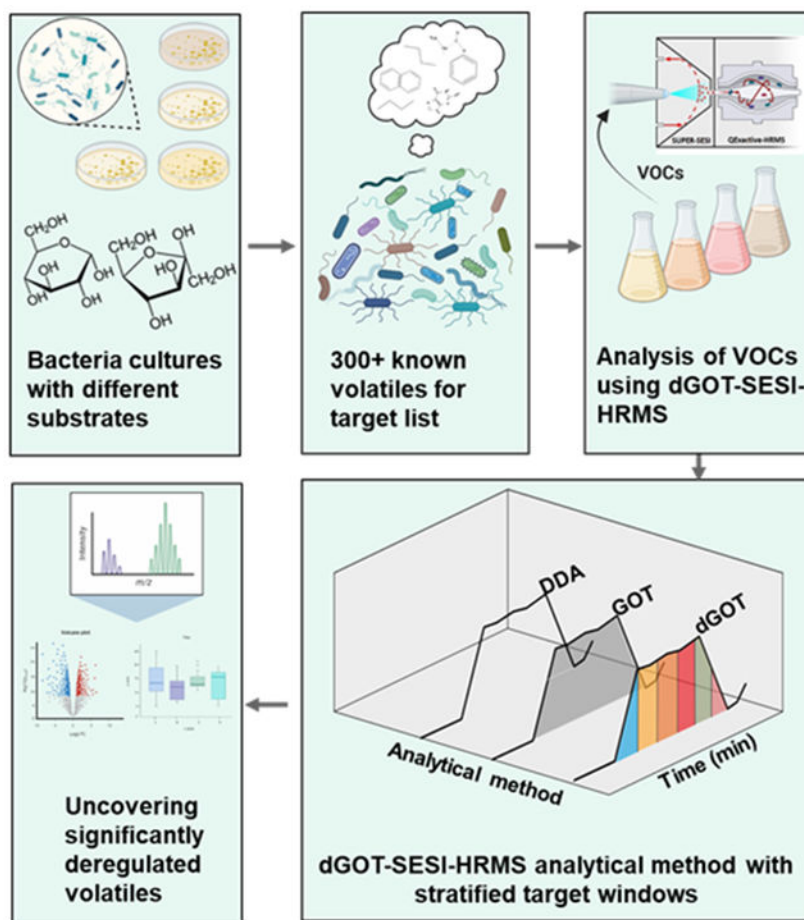
Conceptualization, funding acquisition, project administration, resources, supervision writing – original draft and writing – review and editing, J. Z.; data curation, formal analysis; F. C., R. X., K. M. investigation, methodology writing – original draft and writing – review and editing; F. C., R. X.; critical revision of the manuscript for important intellectual content: all authors. All authors have read and agreed to the published version of the manuscript.

Conflicts of interest

The authors declare no conflict of interest.

demonstrated improved separation of clusters when data was acquired using the dGOT method. Collectively, our dGOT-SESI-HRMS method afforded robust capability of capturing unique VOC profiles from different bacterial strains and culture conditions when compared to conventional GOT and DDA modes, suggesting the newly developed approach can serve as a more reliable analytical method for the sensitive monitoring of gut microbial metabolism.

## Graphical Abstract



## 1. Introduction

Secondary electrospray ionization (SESI) is an emerging mass spectrometry-based analytical technique for the ambient analysis of volatile organic compounds. SESI is able to charge volatiles through a gas-phase chemical ionization mechanism that allows detection of the neutral gaseous analytes,<sup>1</sup> with some reports highlighting SESI's limit of detection to be as low as 0.2 parts per trillion by volume (ppt).<sup>1</sup> Given its modularity, SESI can be coupled with various commercial mass spectrometers, with the most attractive being high-resolution instruments as the improved resolving power offers greater selectivity in feature detection which in turn simplifies metabolite identification.<sup>2,3</sup> Some Orbitrap based SESI platforms further boost the mass spectrometer's ability to detect volatile metabolites in real-time

with resolving powers of  $m/m$  up to 280 000.<sup>3</sup> SESI-based analyses augment our ability to probe the volatilome of biological organisms, which can serve as a complementary technique to conventional metabolomics analyses and further provide deeper insight into metabolic perturbations. The online, non-invasive sampling nature of SESI-high resolution mass spectrometry (HRMS) provides robust feature detection that makes SESI-HRMS ideal for untargeted and targeted volatilomics studies.<sup>4</sup>

Exploring the volatilome has expanded our knowledge of biological systems and has enabled real-time insight into metabolism. Mass spectrometry has been regarded as one of the pivotal analytical methods in metabolomics,<sup>5</sup> and coupling SESI to high resolution mass spectrometers has paved the way for novel VOC based analyses involving breath or bacteria cultures.<sup>6,7</sup> Utilizing SESI-HRMS in an untargeted approach can achieve broad mass coverage for in-depth insight into the biological system. As no established database for SESI-HRMS detected compounds is available, the  $m/z$  features detected would require validation to confirm their chemical identity. The conventional targeted SESI-HRMS approach offers confident identification of the compounds of interest and can provide accurate, quantitative measurements.<sup>8</sup> However, the validation of the targeted compounds is often limited by the availability of authentic standards. To address this technical challenge, a novel approach termed globally optimized targeted (GOT)-MS had been developed which enables reliable metabolic analyses with broad coverage.<sup>9</sup> Meanwhile, in Orbitrap based instruments, sampling volatiles from dense matrices often leads to the simultaneous transfer of a large number of analytes which induces droplet coalescence as well as competition for ionization.<sup>10</sup> This leads to overfilling of the C-trap with the most abundant ions while limiting accumulation of lower abundance ions, in turn rendering the features' intensity below the detection limit. The ion suppression phenomenon will not only limit coverage of prominent VOCs, but also impact SESI-HRMS reproducibility and sensitivity.<sup>11</sup>

Previous results using the GOT-SESI-MS method have proven to be successful in real-time analyses of bacterial volatiles.<sup>12</sup> While untargeted analyses are commonly employed in mass spectrometry, our approach aimed to capitalize on the wealth of knowledge about known bacterial volatiles available in the microbial volatile organic compound (mVOC) database, thereby expanding our analyte coverage.<sup>13</sup> Meanwhile, to overcome the ion competition challenge that hinders the online analyses of volatiles (especially the ones at lower concentration), we also implemented the spectral stitching approach using our curated inclusion lists to mitigate this phenomenon in our real-time queries of bacterial volatiles. Taken together, this study aimed to further develop and optimize a database-assisted, globally optimized targeted (dGOT)-SESI-HRMS analysis method that combined the mVOC database and spectral stitching technique to improve analyte identification and coverage in online analyses of VOCs. Furthermore, we cultured representative anaerobic gut microbes under different nutrient conditions to assess the efficacy of our spectral-stitching supported dGOT-SESI-HRMS method in enhancing current GOT-MS based VOC analysis workflows.

## 2. Materials and methods

### 2.1 Chemicals and reagents

LC-MS grade methanol and acetonitrile as well as analytical grade formic acid were acquired from Fisher Scientific (Hampton, NH, USA). Volatile organic compound quality control (VOCQC) samples were made by diluting chemicals standards of 2-butanone (Alfa Aesar, Haverhill, MA), 2-undecanone (Alfa Aesar, Haverhill, MA), 1-octanol (Acros Organics, Waltham, MA), 2-heptanone (Acros Organics, Waltham, MA), 2-nonanone (Acros Organics, Waltham, MA) in modified Gifu anaerobic medium (mGAM) (HiMedia, West Chester, PA, USA) to monitor instrument performance across experiments. These compounds were selected as they have not been reported in bacterial cultures and thus would not interfere with biological replicates.

### 2.2 Secondary electrospray ionization high resolution mass spectrometry (SESI-HRMS)

An advanced commercially available secondary electrospray ionization (SESI) source, termed SuperSESI (Fossil Ion Tech, Madrid, Spain) was utilized in this study and directly attached to a QExactive™ high-resolution mass spectrometer (HRMS) (Thermo Scientific, San Jose, CA, USA). Prior to the sampling of volatiles, residual VOCs in the system were reduced by baking the sample inlet and ion chamber overnight at 90 °C and 160 °C, respectively. A solution comprising of 0.1% formic acid in water was used as an electrospray solvent and was emitted from a 20 µm non-coated TaperTip capillary (New Objective, Woburn, MA). To examine volatiles from the different cultures' headspace, the SuperSESI source was arranged with previously optimized parameters.<sup>14</sup> Briefly, SESI pressure was fixed at 1 bar and temperatures of sample inlet and ion chamber were respectively set at 70 °C and 90 °C. The mass spectrometer parameters were set as the following: sheath gas flow rate, 60 arbitrary units; auxiliary gas flow rate, 2 arbitrary units; spray voltage, 3.5 kV; ion capillary temperature, 275 °C; and S-lens RF level, 60.0. The mass spectrometer was controlled directly using QExactive™ Tune software (version 2.9) in full MS mode. For both positive and negative ionization modes, the scan range was set from 50 to 500 *m/z*, full MS microscans of 1 ms; automatic gain control (AGC) target of 1e<sup>6</sup> with a high resolving power of 140 000 full width at half maximum (FWHM).

### 2.3 Bacteria culture conditions and analysis of headspace volatiles

Three representative gut bacteria strains, *Bacteroides thetaiotaomicron* (ATCC® 29148™), *Escherichia coli* (ATCC® 25922™), and *Lactobacillus acidophilus* (ATCC® 4356™), were obtained from American Type Culture Collection (ATCC, Manassas, VA). Fecal bacteria isolates (named as gut mix hereafter) were collected from three healthy adult volunteers as reported previously<sup>15</sup> (the protocol approval was obtained from the Institute Review Board, and informed consent was obtained from each individual). All cultures were initially cultured overnight in modified Gifu anaerobic medium (mGAM) (HiMedia, West Chester, PA, USA). The overnight cultures were then inoculated into 20 mL of mGAM medium supplemented with either 1% w/v of sucrose or fructose (Thermo Fisher Scientific, Pittsburgh, PA, USA), and sealed with a three-port GL45 cap. Headspace volatiles were allowed to accumulate overnight at 37 °C in a Coy Laboratories anaerobic chamber (Coy Lab, Flint, Michigan, USA). Ultra-high purity nitrogen gas (99.99%) was used

as a carrier gas to introduce headspace volatiles from bacteria culture samples to the SuperSESI ionization chamber as previously noted.<sup>14</sup> To highlight the robustness of our SESI-HRMS platform, identical experiments were conducted on various non-consecutive days. Experiments were conducted in biological triplicates, with sterile mGAM media void of any active cultures serving as blanks. In addition, reproducibility was ensured by introducing volatile organic compound quality control (VOCQC) samples into the ionization source before and after the tests of biological samples. Final optical density (OD<sub>600</sub>) of bacterial cultures was measured using an ELx808 absorbance plate reader (BioTek, Winooski, VT, USA) to estimate culture growth for normalization.

## 2.4 Data processing and statistical analysis

Preliminary screening of the obtained spectral peaks was achieved using the Quan browser module of Xcalibur version 4.0 (Thermo Fisher Scientific, Waltham, MA, USA). Raw mass spectrometry data was converted into analysis base file (abf) format<sup>16</sup> and imported into MS-DIAL<sup>17</sup> for peak picking and spectral deconvolution. The acquired features were then aligned, and signal intensities were normalized to their respective final culture OD<sub>600</sub>. Individual features were grouped within a mass difference range of 5 ppm to reduce redundancy. To eliminate background signal interference, true peaks were determined with signal-to-noise ratio >3 with respect to culture medium blanks. Spectra that were present in all biological replicates of any culture group were selected for further statistical analysis in efforts to reducing random errors. Statistical analyses, including univariate *T*-test, were conducted using the online resource MetaboAnalyst 5.0.<sup>18</sup> Partial least squares-discriminant analysis (PLS-DA) was utilized to visualize overall headspace chemical profiles of our cultures. Annotation of features was carried out using an in-house developed R code modified from the SODA-MN analysis workflow.<sup>19</sup> Accurate mass tolerance for identification was established with a PPM tolerance of 10 for precursor *m/z*'s. MS/MS fragments were matched to existing databases,<sup>20,21</sup> where spectra that shared at least 4 pairs of matched fragment ions were considered as candidates to calculate spectra similarity. A cosine score cut-off of 70% was used to confirm annotation. These criteria were slightly modified based on previous studies,<sup>22,23</sup> with considerations that a specific SESI-HRMS compound repository has yet been developed and the specific ionization mechanism of SESI-MS remains elusive. In order to enhance the efficiency of analysis and mitigate redundancy, a systematic approach was employed to restrict the annotation of the same volatile compound in both positive and negative ionization modes. This involved the calculation of the neutral mass for similar features, followed by the implementation of a redundancy cut-off threshold of 5 ppm. Consequently, volatile compounds exhibiting a mass difference of less than 5 ppm were excluded from further annotation, thereby minimizing redundancy and ensuring a more focused and streamlined analysis. Data was visualized using GraphPad Prism (GraphPad Software, Inc., San Diego, CA).

## 3. Results and discussion

### 3.1 Developing the dGOT-SESI-HRMS analytical method with spectral stitching

It is well-known that untargeted can simultaneously measure a large number of metabolic features with respect to targeted analyses,<sup>24</sup> yet the large amounts of data generated require

high performance bioinformatics tools to unravel the intricate metabolic networks in the studied biological system.<sup>25</sup> Conversely, one can utilize targeted metabolomics workflows to analyze predefined sets of metabolites with an increased level of precision and accuracy,<sup>26</sup> however, the crux of this analytical approach is the limited metabolome coverage that arises from the finite targeted metabolites typically probed for in the analysis.<sup>27</sup> A unique way to mitigate drawbacks of both strategies is to utilize globally optimized targeted (GOT) approaches by applying both a broad detection of important metabolic features, and then converting the extensive knowledge from existing databases to select pre-defined target analytes that may be of biological importance.<sup>9</sup> While significant strides have been made in unraveling the metabolic pathways of bacteria, it is important to acknowledge that much of their metabolic ties to volatile metabolites remains unexplored. To elucidate the metabolic production of endogenous bacterial volatiles, we sought to further develop the GOT method by curating a list of known bacterial volatiles from the publicly available mVOC database and then incorporating these targets in our GOT based analytical method.<sup>13</sup> The database consisted of 306 unique volatile compounds with detailed information regarding their molecular formula and spectral information systematically collected and organized.<sup>20</sup> Monoisotopic mass for each compound was calculated from the reported molecular formula using an in-house developed MatLab code. For data acquisition, the theoretical  $m/z$  for each compound was used to construct unique inclusion lists to be used in parallel reaction monitoring (PRM) on our Orbitrap instrument.

Meanwhile, efforts have also been made in our study to improve feature stability and analysis reproducibility in SESI-HRMS analyses of volatiles.<sup>28</sup> Despite optimizing the mass spectrometer parameters, it is essential to recognize that ion competition may still impact the reproducibility and sensitivity of volatile analyses, particularly when dealing with complex mixtures of biological origins. Previous reports have suggested that by leveraging the spectral stitching technique, ion competition can be reduced in nano-electrospray mass spectrometry-based analyses of dense matrices.<sup>29,30</sup> The application of this analytical strategy has also been shown to improve metabolic feature detection in Orbitrap based SESI studies of volatiles.<sup>31</sup> Thus, we constructed SESI-based analytical strategies using various staggered  $m/z$  inclusion lists to limit ion competition. To establish the unique target list window, these selected  $m/z$ 's, which serve as representative volatiles from mVOC, were subjected to an ascending sorting algorithm based on their specific predicted monoisotopic mass. Subsequently, a strategically devised staggered arrangement was implemented for each inclusion list to further minimize the likelihood of  $m/z$  value overlap. Each inclusion list was constructed to reflect a minimum  $\pm 1$   $m/z$  between any two consecutively targeted analytes, thereby ensuring accurate and distinct identification of the individual compounds within the complex matrix. In addition, each unique inclusion list was spatially separated, with a minimum duration of 30 seconds for each distinct isolation window. In total, each analytical method lasted a total of 2 minutes. This framework was the foundation for our three unique analytical strategies tested: (i) data dependent acquisition targeting the top 10 most abundant ions (DDA); (ii) inclusion list with no spectral stitching (GOT); (iii) spectral stitching inclusion list with 6 unique inclusion list windows (dGOT) (Fig. 1). DDA was implemented in this study as a reference to conventional data dependent methods, whereas GOT method was used to pinpoint the direct benefits of the spectral

stitching component. Other SESI-HRMS based analyses of volatiles using spectral stitching highlighted comparative performance between 6 and 10 optimized inclusion list windows.<sup>31</sup> Our representative volatile list from mVOC consisted of 306 targets. After comparing the effects between 3 and 6 inclusion list windows, we chose to limit our dGOT method to 6 staggered inclusion list windows to directly lower the mass spectrometer's duty cycle.

### 3.2 Spectral stitching enhances data acquisition in dGOT-SESI-HRMS

Following the method setup, online analysis of volatiles from the headspace of gut microbial cultures was conducted, and partial least squares discriminant analyses (PLS-DA) of the VOC data were generated to summarize the overall headspace chemical profiles among different sample matrix (Fig. S1†). Distinct and tight clustering of the VOC QC samples indicate that the SESI-HRMS platform's analysis was reproducible on multiple days. In addition, independent clustering of the bacterial groups from media blanks confirmed that unique, microbial derived volatiles were actively being emitted into the respective cultures' headspace. Data dependent acquisition (DDA) of the top 10 ions was included as a reference for the performance evaluation of our pseudo-targeted methods. After sampling headspace volatiles from our representative cultures, it was apparent that mVOC relevant MS features detected in our analysis were proportional to the number of inclusion list windows employed during the spectral stitching setup (Fig. 2A), with a cumulative 109 features detected (and with MS/MS spectrum collected) using our dGOT method. In comparison, one inclusion list without spectral stitching only provided 54 features with MS/MS information collected. DDA method did not provide many useful features, with a total of 4 MS/MS peaks detected in both ionization modes when trying to match the globally targeted mVOC compounds. To ensure that the analyzed peaks were in fact bacterial derived volatiles, a signal-to-noise ratio >3 (bacterial culture *vs.* medium) was used to confirm all background peaks from media are eliminated from the analysis. Consistent with our earlier findings, the number of true peaks (after applying the aforementioned signal-to-noise cut off) derived from our bacterial cultures increased from 4 in the DDA method to 48 in the GOT method (Fig. 2B). The most robust data acquisition was demonstrated when analyzing headspace volatiles using the stratified dGOT method with a total of 88 features deemed true peaks. In addition, we conducted a performance comparison with a modified dGOT approach featuring 3 inclusion list windows. Our results aligned with expectations, as the number of windows exhibited a direct proportionality with the detected peaks. Specifically, we successfully acquired a total of 77 MSMS peaks, out of which 55 were confirmed as true peaks when utilizing the 3-window dGOT method (Fig. S2†). Collectively, our data suggested that the increased duty cycle with spectral stitching approach could lead to enhanced data collection efficiency. Thus, our analyses were conducted with spectral stitching of 6 inclusion list windows.

---

†Electronic supplementary information (ESI) available: Fig. S1: PLS-DA summarizing the differences in headspace chemical profiles among our bacteria cultures, media blanks and VOCQC samples. Fig. S2: Summary of dGOT method performance when incorporating three unique target list windows. Fig. S3: Representative head to tail spectra of annotated MSMS features from dGOT-SESI-HRMS analysis of bacterial headspace volatiles. Fig. S4: Principal component analyses summarizing each of DDA, GOT and DGOT method's respective ability at distinguishing the volatile differences between GutMix and each representative strain supplemented with sucrose. Fig. S5: Heatmap summarizing the relative abundance of the annotated features detected with the dGOT method across all of our culture groups. See DOI: <https://doi.org/10.1039/d3an01487h>

### 3.3 dGOT-SESI-HRMS enables improved annotation of gut microbial volatiles

The identification of the culture derived volatile features could enable additional insights into their biochemical origins. While a widely accepted database for the annotation of SESI-HRMS acquired volatiles is yet to be developed, it is possible to leverage curated spectral information available in established public databases to annotate the MS/MS peaks. Herein, we extracted spectral information from the mVOC database when available, in combination with fragmentation patterns of chemical standards reported in other established databases such as PubChem and HMDB.<sup>20,21</sup> Annotation was confirmed using a minimum of 4 fragment ions matched with a PPM cutoff of 10 with respect to the standard spectra and a cosine score cutoff of 70% for increased confidence in compound identity. Given the low number of acquired MSMS features, analysis of volatiles with the DDA method resulted in a single identifiable compound (Fig. 3A). A gradual and incremental increase of annotated metabolic features was apparent when inclusion list windows were added, with a total of 15 and 25 unique volatiles annotated in our GOT and dGOT methods, respectively. In comparison, the 3-window dGOT method allowed for annotation of 22 unique volatiles (Fig. S2<sup>†</sup>). As expected with improved data acquisition, our optimized dGOT method allowed for superior annotation of volatiles. Head-to-tail spectra of dodeca-2-one (Fig. 3B), a ketone detected in our analysis of headspace volatiles with a cosine score of 0.83, is provided as reference for annotation. Similarly, 4-hydroxybenzenesulfonicacid was also annotated with a cosine score of 0.88 (Fig. 3C). A full list of the annotated volatiles from our dGOT method is summarized in Table 1, including chemical class, chemical formula, and cosine score. Table 1 also includes relative change of abundance between our fructose and sucrose supplemented cultures. Additional representative head to tail spectra of annotated compounds are presented in Fig. S3.<sup>†</sup> The annotated compounds encompassed various chemical classes such as carboxylic acids, ketones, and alcohols among others, showcasing that a SESI-HRMS based screening platform is able to acquire data from a broad range of chemicals.

While the diversity of the detected VOC classes is dependent on the heterogeneity of bacterial cultures, the abundance of unique chemical groups suggests a broadened coverage achieved by dGOT-SESI-HRMS. SESI-HRMS analyses of volatiles have applied feature-based analyses for biological interpretation.<sup>32</sup> Herein, our dGOT-SESI-HRMS method can further corroborate those findings by offering putative identification of the analytes. Our analysis was able to detect decan-1-ol, 1*H*-pyrrole and propanamide in our samples, which were also reported to be associated with EC when analyzed with gas chromatography-mass spectrometry.<sup>33-35</sup> Of the annotated volatiles, 5-methyl-oxolan-2-one was reported before by GC-MS analyses of fecal headspace samples collected from donors subjected to iron supplementation.<sup>36</sup> Given that the fecal metabolome can potentially serve as functional readout of host metabolism,<sup>37</sup> we expect in future studies dGOT-SESI-HRMS could also be leveraged for reliable and non-invasive screening of fecal samples to predict meolic status of patients.

### 3.4 dGOT-SESI-HRMS improves volatilome analyses and uncovers substrate and strain associated altered volatiles

The online nature of SESI analyses has rendered it a viable tool for the analyses of real time VOCs in various biological systems.<sup>38-42</sup> SESI-HRMS platforms have been successfully utilized for monitoring changes in the yeast volatilome,<sup>43</sup> segregating bacterial cultures using the chemical composition of their culture headspace,<sup>12</sup> as well as enabling queries of lung cancer cells treated with cisplatin.<sup>44</sup> Here, we aimed to utilize principal component analysis to assess if our newly developed dGOT-SESI-HRMS method improves our ability of distinguishing nutrient substrate contributed changes to the metabolic outcomes of gut microbes using their headspace VOC profiles. We cultured representative bacteria strains *Bacteroides thetaiotaomicron* (BT), *Escherichia coli* (EC), *Lactobacillus acidophilus* (LB), and GutMix (GM) for this analysis. Given that the microbial metabolic processes are dependent on nutrient availability,<sup>45</sup> we conducted experiments using identical bacteria strains supplemented with either fructose or sucrose as the energy substrate. Fructose can be readily metabolized by bacteria for energy metabolism, whereas sucrose is a disaccharide composed of both glucose and fructose linked by a glycosidic bond. By doing so, we aimed to gain valuable insights into the method's capability to differentiate the volatile profiles influenced by distinct energy substrates.

Utilizing PCA, we summarized the performance of each analytical method employed in distinguishing the volatile changes among our representative strains. When comparing the headspace volatiles of our strains cultured with either fructose or sucrose using the DDA method, we observed overlap between each substrate condition for all of the bacterial strains cultured (Fig. 4). Limited improvement in PCA clustering was evident when utilizing the GOT method for data acquisition, suggesting inadequate analytical performance while we intend to uncover substrate level changes in the volatile profile. However, upon collecting volatiles with the optimized dGOT method, we observed distinct clustering among all of our identical strains cultured with either fructose or sucrose as energy substrates. This finding underscores the capability of our optimized analytical method in distinguishing substrate-level differences in the headspace of our bacterial strains. When considering that each molecule of sucrose contains one molecule of fructose linked to one glucose, it is reasonable to anticipate an inherent overlap in the metabolic pathways responsible for their breakdown after our representative microbes digest the glycosidic bond.<sup>46</sup> These results provide crucial insights into the efficacy of our dGOT method in capturing the distinction of volatile profiles between bacterial cultures subjected to different energy substrates.

After confirming the method's ability at identifying substrate level differences in the volatilome, we sought to determine if our optimized dGOT method is capable of identifying strain level differences between bacteria cultured with a similar energy substrate. To achieve this, we compared each analytical methods' performance at identifying strain level differences between GutMix and each representative strain cultured with sucrose. When comparing the DDA method's capability to discern unique volatiles in the bacteria's headspace, we observed overlap among all representative bacterial strains when compared to GutMix (Fig. S4†). Upon incorporating a target inclusion list, as seen in the GOT method, we noted a moderate improvement in the clustering of the groups in PCA. However, it was

when we applied the dGOT method that we witnessed an enhancement in the separation between the groups. Although some overlap was still present in between the single strains and GutMix, the dGOT method displayed the least amount of group overlap in PCA, suggesting its ability to distinguish strain-level changes among bacteria-derived volatiles in the headspace. An interesting observation was the overlap of strains with the GutMix group when comparing the performance of all our analytical methods. We attribute this to the complexity of the human microbiome, which comprises a multitude of bacterial strains. The GutMix contains active growth of the individually cultured strains analyzed, such as LB and EC, leading to partial similarities in the volatile profiles of the cultures, hence the observed overlap. These findings shed light on the advantages of the dGOT method in effectively unraveling strain-specific variations in bacterial-derived volatiles, providing valuable insights into the metabolic intricacies of the microbial community under different culture conditions.

To further demonstrate the analytical capability of our dGOT method, we aimed to capture the metabolic adaptability of gut microbes using our dGOT-SESI-HRMS approach. Specifically, we sought to dig deeper into the volatile profiles of identical bacterial strains supplemented with different energy substrates. The volatile profiles of all of our experimental groups were compared using a partial least squares discriminant analysis (PLS-DA), where we observed independent clustering between all analyzed groups (Fig. 5A). The dGOT method enables us to unravel subtle metabolic shifts within the gut microbes, providing valuable insights into their adaptability and responses to distinct environmental conditions. This result highlights the robust discriminatory power of our analytical approach in effectively separating the volatile profiles of different bacterial strains under distinct culture conditions. A summary of the relative abundance of the annotated features detected with the dGOT method is shown in the heatmap in Fig. S5.† Furthermore, to showcase the analytical prowess of our newly developed dGOT method, we compared its ability to uncover significantly altered features between strains cultured with different substrates. In this analysis, the DDA method was only able to identify a single significantly altered volatile feature for each of the four representative strains (Fig. 5B). The GOT method exhibited a modest improvement, identifying 4 significantly altered features among our strains. As anticipated, the dGOT method showcased a notably superior performance in uncovering altered volatiles, revealing a total of 33 significantly altered VOCs across our strains ( $p$ -value  $<0.05$ ). In similar fashion, when comparing the ability of our methods at providing prominently altered features driving separation of PLS-DA models, we also observed a similar trend in the data. When deploying a pair-wise analysis of the strains cultured with either fructose or sucrose, DDA revealed 17 features that demonstrated a VIP score  $>1$  (Fig. 5C). The addition of an inclusion list in the GOT method improved the number of VIP features to 80. Overall, the dGOT method still fared the best, with a total of 133 features with a VIP score  $>1$  detected across our culture groups. These findings emphasize the enhanced sensitivity and accuracy of our dGOT method in detecting subtle changes in the volatile profiles of bacterial strains cultured with different energy substrates. The ability to identify a larger number of altered VOCs further underscores the potential of our method in elucidating the metabolic adaptability and responses of gut microbes to varying environmental conditions.

As our dGOT method was able to detect an increased number of significantly altered features among our representative bacteria strains cultured in either fructose or sucrose, we sought to determine if the annotated volatiles could provide valuable insight into the chemical nature of volatiles produced by bacteria. Upon analyzing the differences between our cultures supplemented with either fructose or sucrose using an enrichment analysis, it was evident that fatty esters were the most enriched chemical class in our bacteria cultures ( $p$ -value =  $4.92 \times 10^{-4}$ ). While the metabolic mechanisms responsible for endogenous VOC synthesis are still being uncovered, we believe that our optimized dGOT approach enables advances in our understanding of microbial metabolism and paves the way for more comprehensive investigations in microbial metabolism studies.

#### 4. Conclusion

In summary, this study introduced a new SESI-HRMS based analytical strategy, spectral stitching supported dGOT-SESI-HRMS, for enhanced analyses of gut microbial VOCs. The dGOT-SESI-HRMS retains the advantages of targeted detection for a broader VOC metabolite coverage while leverage known microbial VOC database for meaningful volatile detection. Implementation of the spectral stitching technique proved vital to improve the detection sensitivity of targeted VOCs by allowing analyses to focus on low abundance volatiles that would have been suppressed when using DDA methods. Additionally, staggering the inclusion list windows in the dGOT method *via* spectral stitching reduces ion competition with respect to the single window used in traditional GOT methods, and further improves the performance of SESI-based analyses in probing analyte dense matrices. Our method demonstrated a strong capability in semi-global profiling to elucidate the volatile differences in headspace of unique gut bacterial strains and culture conditions. Importantly, as an established spectral database for SESI-HRMS analyses of volatiles has yet to be developed, dGOT-SESI-HRMS provides a novel approach to leverage the existing knowledgebase for improved annotation of volatile features. Collectively, our newly developed dGOT-SESI-HRMS strategy can play a prominent role in many future volatilomics studies by increasing the overall coverage of the volatilome, enhancing the identification of unknowns, and improving the sensitivity and quantitative performance of analysis to enable improved biological interpretation that is complementary to existing techniques.

#### Supplementary Material

Refer to Web version on PubMed Central for supplementary material.

#### Acknowledgements

Research reported in this publication was supported by the National Institute of General Medical Sciences of the National Institutes of Health under award number R35GM133510 awarded to J. Z. The content is solely the responsibility of the authors and does not necessarily represent the official views of the National Institutes of Health.

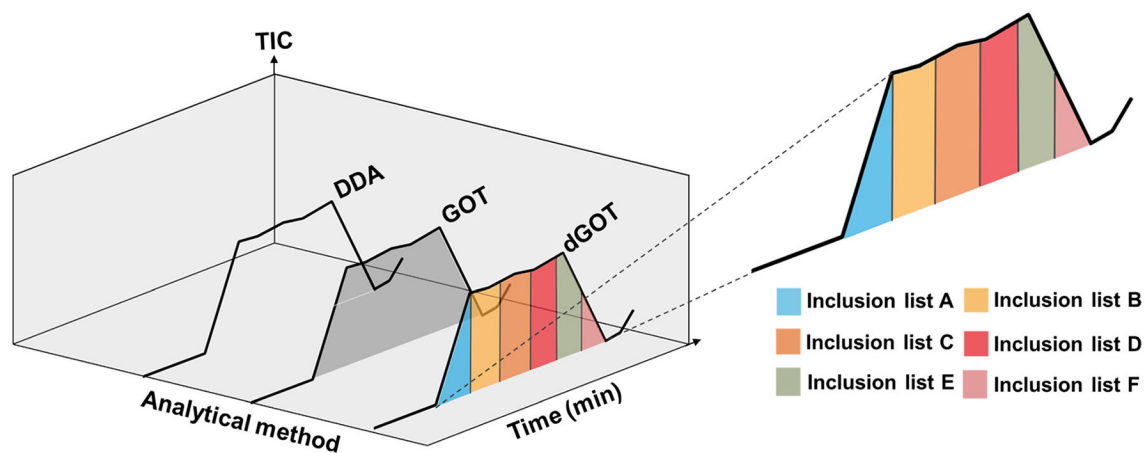
## Data availability

All data supporting the conclusions of this manuscript are provided in the text and figures. Please contact the author for data requests.

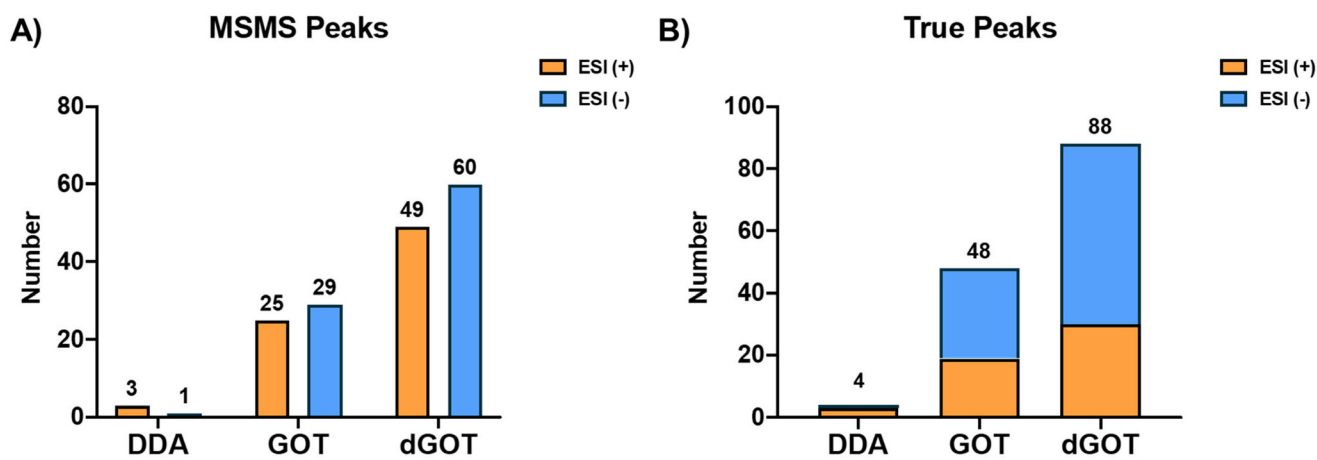
## References

1. Martínez-Lozano Sinues P, Rus J, de la Mora GF, Hernández M and de la Mora J. Fernández, J. Am. Soc. Mass Spectrom, 2009, 20, 287–294. [PubMed: 19013080]
2. Kornilova TA, Ukolov AI, Kostikov RR and Zenkevich IG, Rapid Commun. Mass Spectrom, 2013, 27, 461–466. [PubMed: 23280978]
3. Bruderer T, Gaugg MT, Cappellin L, Lopez-Hilfiker F, Hutterli M, Perkins N, Zenobi R and Moeller A, J. Am. Soc. Mass Spectrom, 2020, 31(8), 1632–1640.
4. Bean HD, Zhu J and Hill JE, J. Visualized Exp, 2011, 2664, DOI: 10.3791/2664.
5. Kim YM and Heyman HM, Methods Mol. Biol, 2018, 1775, 107–118. [PubMed: 29876813]
6. Bean HD, Zhu J and Hill JE, J. Visualized Exp, 2011, 52, e2664.
7. Schwarz EI, Martínez-Lozano Sinues P, Bregy L, Gaisl T, Garcia Gomez D, Gaugg MT, Suter Y, Stebler N, Nussbaumer-Ochsner Y, Bloch KE, Stradling JR, Zenobi R and Kohler M, Thorax, 2016, 71, 110–117. [PubMed: 26671307]
8. García-Gómez D, Bregy L, Nussbaumer-Ochsner Y, Gaisl T, Kohler M and Zenobi R, Environ. Sci. Technol, 2015, 49, 12519–12524. [PubMed: 26390299]
9. Shi X, Wang S, Jasbi P, Turner C, Hrovat J, Wei Y, Liu J and Gu H, Anal. Chem, 2019, 91, 13737–13745. [PubMed: 31556994]
10. Sarvin B, Lagziel S, Sarvin N, Mukha D, Kumar P, Aizenshtein D and Shlomi T, Nat. Commun, 2020, 11, 3186. [PubMed: 32581242]
11. Kaufmann A and Walker S, Rapid Commun. Mass Spectrom, 2018, 32(6), 503–515. [PubMed: 29297948]
12. Li H and Zhu J, Anal. Chem, 2018, 90, 12108–12115. [PubMed: 30240565]
13. Lemfack MC, Gohlke BO, Toguem SMT, Preissner S, Piechulla B and Preissner R, Nucleic Acids Res., 2018, 46, D1261–d1265. [PubMed: 29106611]
14. Lee JHJ and Zhu J, Metabolites, 2020, 10, 351. [PubMed: 32872254]
15. Zhang S, Xu M, Sun X, Liu X, Choueiry F, Xu R, Shi H and Zhu J, J. Chromatogr. B: Anal. Technol. Biomed. Life Sci, 2022, 1188, 123027.
16. Tsugawa H, Kanazawa M, Ogiwara A and Arita M, Bioinformatics, 2014, 30, 2379–2380. [PubMed: 24753485]
17. Tsugawa H, Cajka T, Kind T, Ma Y, Higgins B, Ikeda K, Kanazawa M, VanderGheynst J, Fiehn O and Arita M, Nat. Methods, 2015, 12, 523–526. [PubMed: 25938372]
18. Pang Z, Chong J, Zhou G, de Lima Morais DA, Chang L, Barrette M, Gauthier C, Jacques PE, Li S and Xia J, Nucleic Acids Res., 2021, 49, W388–W396. [PubMed: 34019663]
19. Xu R, Lee J, Zhang S, Chen L and Zhu J, Anal. Chim. Acta, 2022, 1221, 340145. [PubMed: 35934377]
20. Kim S, Chen J, Cheng T, Gindulyte A, He J, He S, Li Q, Shoemaker BA, Thiessen PA, Yu B, Zaslavsky L, Zhang J and Bolton EE, Nucleic Acids Res., 2021, 49, D1388–D1395. [PubMed: 33151290]
21. Wishart DS, Feunang YD, Marcu A, Guo AC, Liang K, Vazquez-Fresno R, Sajed T, Johnson D, Li C, Karu N, Sayeeda Z, Lo E, Assempour N, Berjanskii M, Singhal S, Arndt D, Liang Y, Badran H, Grant J, Serra-Cayuela A, Liu Y, Mandal R, Neveu V, Pon A, Knox C, Wilson M, Manach C and Scalbert A, Nucleic Acids Res., 2018, 46, D608–D617. [PubMed: 29140435]
22. Tsugawa H, Satoh A, Uchino H, Cajka T, Arita M and Arita M, Metabolites, 2019, 9(6), 119. [PubMed: 31238512]
23. Schlotterbeck J, Chatterjee M, Gawaz M and Lämmerhofer M, Anal. Chim. Acta, 2019, 1046, 1–15. [PubMed: 30482286]

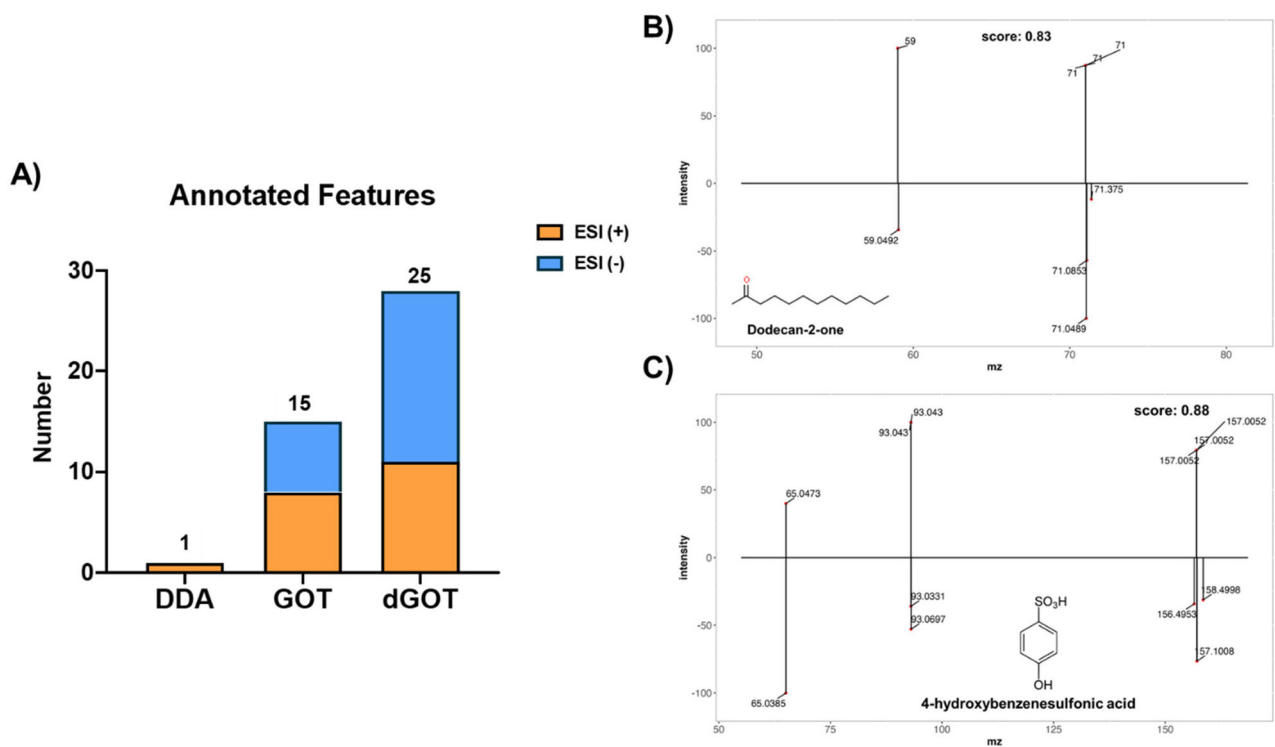
24. Schrimpe-Rutledge AC, Codreanu SG, Sherrod SD and McLean JA, *J. Am. Soc. Mass Spectrom.*, 2016, 27, 1897–1905. [PubMed: 27624161]
25. Cajka T and Fiehn O, *Anal. Chem.*, 2016, 88, 524–545. [PubMed: 26637011]
26. Alonso A, Marsal S and Julià A, *Front. Bioeng. Biotechnol.*, 2015, 3, 23. [PubMed: 25798438]
27. Gu H, Zhang P, Zhu J and Raftery D, *Anal. Chem.*, 2015, 87, 12355–12362. [PubMed: 26579731]
28. Singh KD, Tancev G, Decrue F, Usemann J, Appenzeller R, Barreiro P, Jauma G, Macia Santiago M, Vidal de Miguel G, Frey U and Martínez-Lozano Sinues P, *Anal. Bioanal. Chem.*, 2019, 411, 4883–4898. [PubMed: 30989265]
29. Southam AD, Weber RJ, Engel J, Jones MR and Viant MR, *Nat. Protoc.*, 2016, 12, 310–328. [PubMed: 28079878]
30. Kaufmann A and Walker S, *Rapid Commun. Mass Spectrom.*, 2016, 30, 1087–1095. [PubMed: 27003046]
31. Lan J, Kaeslin J, Greter G and Zenobi R, *Anal. Chim. Acta*, 2021, 1150, 338209. [PubMed: 33583550]
32. Li S, Park Y, Duraisingham S, Strobel FH, Khan N, Soltow QA, Jones DP and Pulendran B, *PLoS Comput. Biol.*, 2013, 9, e1003123. [PubMed: 23861661]
33. Fitzgerald S, Duffy E, Holland L and Morrin A, *Sci. Rep.*, 2020, 10, 17971. [PubMed: 33087843]
34. Ramírez-Guizar S, Sykes H, Perry JD, Schwalbe EC, Stanforth SP, Perez-Perez MCI and Dean JR, *J. Chromatogr. A*, 2017, 1501, 79–88. [PubMed: 28438317]
35. Karami N, Mirzajani F, Rezadoost H, Karimi A, Fallah F, Ghassempour A and Aliahmadi A, *F1000Research*, 2017, 6, 1415. [PubMed: 29375811]
36. Ahmed A, Slater R, Lewis S and Probert C, *Molecules*, 2020, 25(21), 5113. [PubMed: 33153225]
37. Zierer J, Jackson MA, Kastenmüller G, Mangino M, Long T, Telenti A, Mohnhey RP, Small KS, Bell JT, Steves CJ, Valdes AM, Spector TD and Menni C, *Nat. Genet.*, 2018, 50, 790–795. [PubMed: 29808030]
38. Choueiry F and Zhu J, *Anal. Chim. Acta*, 2021, 339230, DOI: 10.1016/j.aca.2021.339230. [PubMed: 34815037]
39. Li H, Xu M and Zhu J, *Anal. Chem.*, 2019, 91, 854–863. [PubMed: 30516360]
40. Zhu J and Hill JE, *Food Microbiol.*, 2013, 34, 412–417. [PubMed: 23541210]
41. Mengers HG, Schier C, Zimmermann M, Gruhlke MCH, Block E, Blank LM and Slusarenko AJ, *Food Chem.*, 2022, 397, 133804. [PubMed: 35932686]
42. Gómez-Mejía A, Arnold K, Bär J, Singh KD, Scheier TC, Brugger SD, Zinkernagel AS and Sinues P, *iScience*, 2022, 25, 105080. [PubMed: 36157573]
43. Tejero Rioseras A, Garcia Gomez D, Ebert BE, Blank LM, Ibáñez AJ and Sinues PM, *Sci. Rep.*, 2017, 7, 14236. [PubMed: 29079837]
44. Choueiry F and Zhu J, *Anal. Chim. Acta*, 2021, 1189, 339230. [PubMed: 34815037]
45. Choueiry F, Xu R and Zhu J, *J. Proteome Res.*, 2022, 21, 470–481. [PubMed: 35043624]
46. Holscher HD, *Gut Microbes*, 2017, 8, 172–184. [PubMed: 28165863]



**Fig. 1.** Schematic of dGOT-SESI-HRMS analytical strategy with spectral stitching inclusion windows; total ion chromatogram depicting relative increase of ions over time as volatiles are carried in to the SUPERSESI source. Each chromatogram highlights either traditional GOT or each individual dGOT method, with colors reflecting the unique inclusion list windows for acquisition. Each colored window consisted of unique PRM inclusion lists used for targeting VOCs of interest.



**Fig. 2.** Comparison of dGOT-SESI-HRMS method performance with respect to the traditional GOT and DDA methods, (A) number of MS/MS peaks detected in each method in both positive and negative ionization modes and (B) the true MS/MS peaks with signal-to-noise ratio >3.



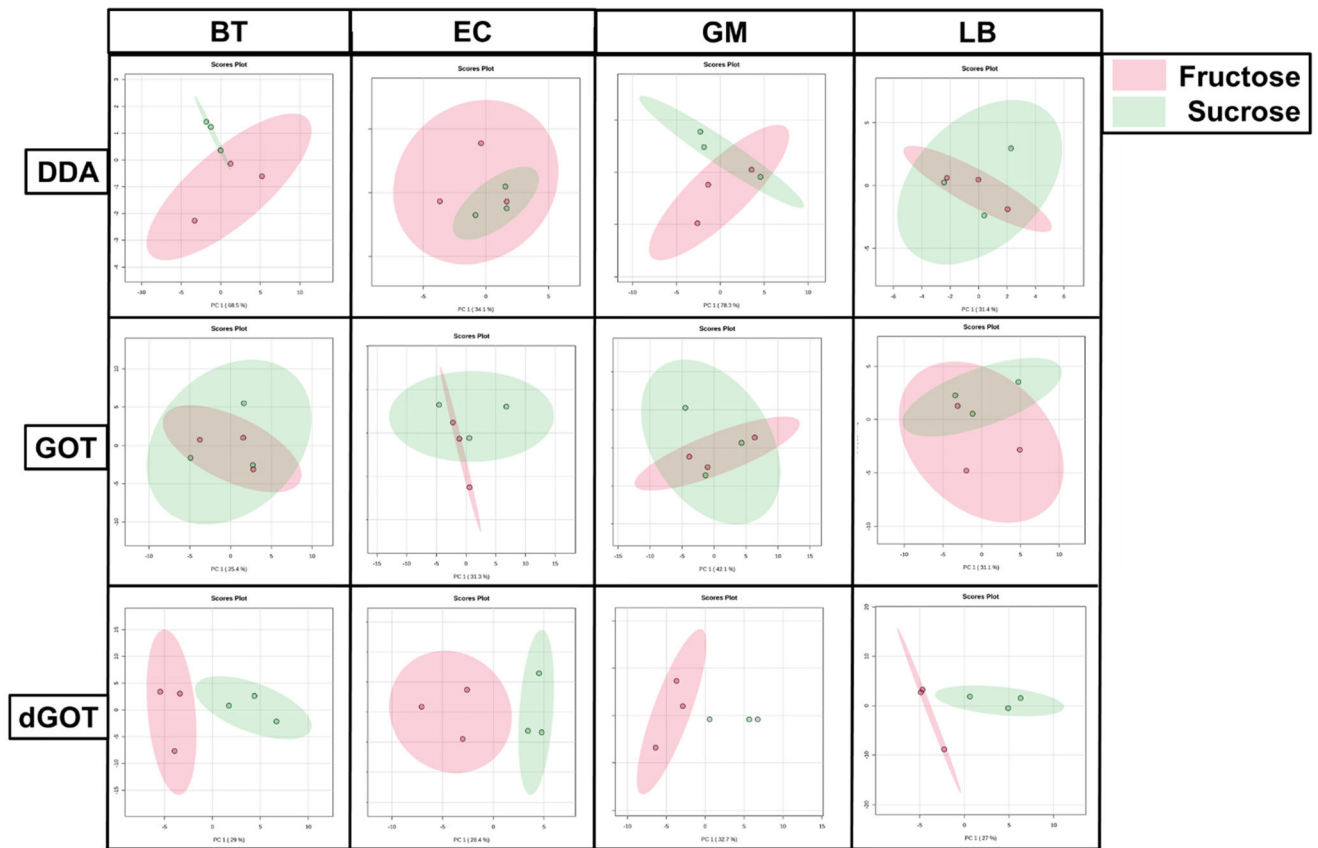


**Fig. 4.** Principal component analysis (PCA) summarizing the ability of our dGOT method to uncover the differences in headspace chemical profiles among our 4 representative bacteria strains cultured with either fructose or sucrose.

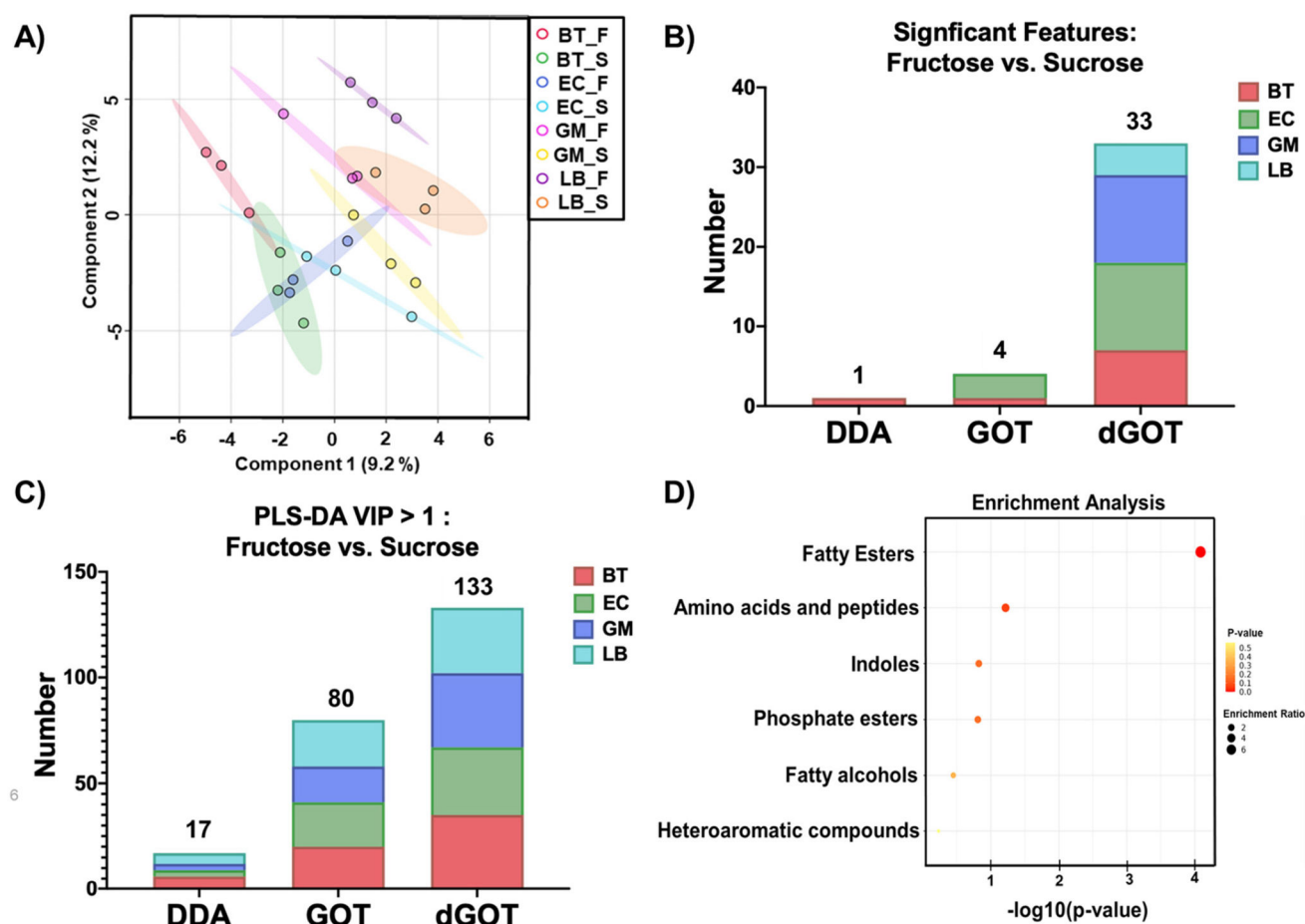


**Fig. 5.** (A) Partial least squares discriminant analysis (PLS-DA) summarizing the differences in headspace chemical profiles of all of our representative bacteria strains cultured with either sucrose or fructose and analyzed using the dGOT analysis method. (B) Increase in the total number of significantly altered VOCs in the headspace of our bacteria cultures supplemented with sucrose and fructose cultures when analyzed with the dGOT method. (C) Increase in the total number of bacteria VOCs with VIP score >1 in their respective PLS-DA models comparing substrate conditions when analyzed with the dGOT method. (D) Enrichment analysis highlighting fatty esters as a significantly altered chemical class in our bacteria cultures supplemented with fructose with respect to sucrose.

Annotated MS/MS features in our representative cultures supplemented with fructose vs. sucrose when analyzed with the optimized dGOT analytical method, with their respective classes, molecular formulas and relative degree of change

Table 1

| Compound name                                       | <i>m/z</i> | Cosine score | Class                         | Formula  | Fruc/Suc |
|---|------------|--------------|-------------------------------|--|----------|
| ( <i>B</i> )-But-2-enoic acid                       | 87.0438    | 0.72         | Acids                         | C <sub>4</sub> H <sub>6</sub> O <sub>2</sub>   | ↓        |
| (Methyltetrasulfanyl)methane                        | 156.9307   | 0.92         | Thioethers                    | C <sub>2</sub> H <sub>6</sub> S <sub>4</sub>   | ↑        |
| (Methyltrisulfanyl)methane                          | 126.971    | 0.77         | Sulfides                      | C <sub>2</sub> H <sub>6</sub> S <sub>3</sub>   | ↑        |
| 1-(1,3-Thiazol-2-yl)ethanone                        | 128.0162   | 0.70         | Nitrogen containing compounds | C <sub>3</sub> H <sub>5</sub> NOS              | ↓        |
| 1-(2-Hydroxyphenyl)ethanone                         | 135.0435   | 0.87         | Ketones                       | C <sub>8</sub> H <sub>8</sub> O <sub>2</sub>   | ↓        |
| 1-(4-Methoxyphenyl)ethanone                         | 149.0587   | 0.94         | Ethers                        | C <sub>9</sub> H <sub>10</sub> O <sub>2</sub>  | ↓        |
| 1,3,5-Trimethylbenzene                              | 121.102    | 0.85         | Alkylbenzenes                 | C <sub>9</sub> H <sub>12</sub>                 | ↓        |
| 1,3-Thiazole  | 86.0055    | 0.73         | Nitrogen containing compounds | C <sub>3</sub> H <sub>3</sub> NS               | ↓        |
| 13-Methyltridecanoic acid                           | 241.215    | 0.75         | Acids                         | C <sub>15</sub> H <sub>30</sub> O <sub>2</sub> | ↓        |
| 1 <i>H</i> Pyrrrole                                 | 68.0492    | 0.73         | Nitrogen containing compounds | C <sub>4</sub> H <sub>5</sub> N                | ↓        |
| 2-Methyl-5-propan-2-ylcyclohexa-2,5-diene-1,4-dione | 163.075    | 0.84         | Quinones                      | C <sub>10</sub> H <sub>12</sub> O <sub>2</sub> | ↓        |
| 3-Hydroxybutan-2-one                                | 89.0592    | 0.76         | Alcohols                      | C <sub>4</sub> H <sub>8</sub> O <sub>6</sub>   | ↓        |
| 3-Methyl-1 <i>H</i> -indole                         | 130.0652   | 0.93         | Indoles                       | C <sub>9</sub> H <sub>9</sub> N                | ↑        |
| 5-Ethylloxolan-2-one                                | 113.0589   | 0.85         | Lactones                      | C <sub>6</sub> H <sub>10</sub> O <sub>2</sub>  | ↑        |
| 5-Heptyloxolan-2-one                                | 185.1534   | 0.75         | Lactones                      | C <sub>11</sub> H <sub>20</sub> O <sub>2</sub> | ↓        |
| 5-Hexyloxolan-2-one                                 | 169.1217   | 0.85         | Lactones                      | C <sub>10</sub> H <sub>18</sub> O <sub>2</sub> | ↓        |
| 5-Methylloxolan-2-one                               | 99.04353   | 0.96         | Lactones                      | C <sub>5</sub> H <sub>8</sub> O <sub>2</sub>   | ↓        |
| Decan-1-ol  | 159.1761   | 0.74         | Alcohols                      | C <sub>10</sub> H <sub>22</sub> O              | ↑        |
| Dodecan-2-one                                       | 183.1723   | 0.89         | Ketones                       | C <sub>12</sub> H <sub>24</sub> O              | ↓        |
| Furan-2-ylmethyl 3-methylbutanoate                  | 181.0835   | 0.84         | Furans                        | C <sub>10</sub> H <sub>14</sub> O <sub>3</sub> | ↓        |
| Methyl 2-hydroxybenzoate                            | 151.0391   | 0.72         | Ester                         | C <sub>8</sub> H <sub>8</sub> O <sub>3</sub>   | ↓        |
| Methyl 3-methylbutanoate                            | 117.0906   | 0.81         | Furans                        | C <sub>10</sub> H <sub>14</sub> O <sub>3</sub> | ↓        |
| Methyl hexanoate                                    | 131.1064   | 0.96         | Ester                         | C <sub>7</sub> H <sub>14</sub> O <sub>2</sub>  | ↓        |
| Octan-1-ol  | 129.1277   | 0.75         | Alcohols                      | C <sub>8</sub> H <sub>18</sub> O               | ↑        |
| Propanamide   | 72.04491   | 0.75         | Nitrogen compounds            | C <sub>3</sub> H <sub>7</sub> ON               | ↓        |

↑ denotes increase in fructose group while ↓ denotes increase in sucrose groups.

Author Manuscript

Author Manuscript

Author Manuscript

Author Manuscript